Study of the Cu-Au and Ag-Au Alloy Systems as a Function of Composition and Order through the Use of the Mössbauer Effect for ^{197}Au†

Paul G. Huray* and Louis D. Roberts‡
Oak Ridge National Laboratory, Oak Ridge, Tennessee 37830,
University of Tennessee, Knoxville, Tennessee 37916,
and University of North Carolina, Chapel Hill, North Carolina 27514

and

J. O. Thomson
Oak Ridge National Laboratory, Oak Ridge, Tennessee 37830
and University of Tennessee, Knoxville, Tennessee 37916
(Received 9 March 1971)

Mössbauer spectra for ^{197}Au and the alloy electrical resistivities have been measured for ordered and disordered phases of Cu-Au and Ag-Au alloys. The alloy compositions span the complete range ($\sim$ 0–100)% Au. The change of isomer shift with pressure between $\sim$ 0 and 65 kbar has also been measured for ordered Cu_3Au. A theoretical model is given which describes the isomer shift in terms of the average atomic volume of the alloy, the short-range-order parameters, and the alloy composition. The agreement between the model and our measurements is good. Friedel oscillations are shown to be present in the electron charge distribution in these alloys. An estimate of the relative contributions of alloy-volume and short-range-order effects to the average electron charge density at the gold nuclei is given.

I. INTRODUCTION

To illustrate the nature and objectives of the measurements to be described below, let us imagine a face-centered-cubic (fcc) alloy of metals x and y and, for example, of composition x_3y. For simplicity in this illustration we will suppose that the alloy may be prepared in either an ordered or in a completely disordered state. In the ordered state, x atoms will occupy face sites and y atoms will occupy corner sites in the alloy unit cell. We shall assume, too, that the average electron charge density over all of the y nuclei, $\langle|\psi_y(0)|^2\rangle$, can be measured. At a particular y nucleus the charge density $|\psi_y(0)|^2$ may be associated, in part, specifically with the y atom itself and, in part, with contributions to be associated with the neighboring atoms. Thus, for the ordered alloy, the nearest-neighbor contribution to $\langle|\psi_y(0)|^2\rangle$ will be due to twelve x atoms, the next-nearest-neighbor contribution will be due to six y atoms, etc. If, however, the alloy is completely disordered, the nearest-neighbor contribution to $\langle|\psi_y(0)|^2\rangle$ will now be due to nine x and to three y atoms, the next-nearest-neighbor contribution will be due to 4.5 x and 1.5 y atoms, etc. Thus the change of $\langle|\psi_y(0)|^2\rangle$ due to this change of atomic order will correspond to replacing three x atoms by y atoms in the nearest-neighbor shell; to replacing 4.5 y atoms by x atoms in the next-nearest-neighbor shell, etc. It is our purpose here to present measurements of $\langle|\psi_y(0)|^2\rangle$ and to show, through an approximate theoretical model, how this charge density depends on alloy composition, atomic volume, and on changes of neighbor configuration such as those described in the above illustration. Through this theoretical model, information is obtained about radial electron charge density distributions surrounding the x and y atoms.

We describe, then, a study of the electron charge density distributions for two binary-alloy systems as a function of alloy composition and of short-range order. The charge density measurements have been made through the use of the Mössbauer effect[1] for ^{197}Au, and we have investigated the Cu-Au and Ag-Au systems over the entire range of compositions. As will be seen, these systems are particularly suitable for this present study because of the contrasting ways in which short-range order and average atomic volume depend on alloy composition and heat treatment.[2–7] For the fcc Ag-Au system the average atomic volume displays relatively little dependence on composition and only disordered alloys may be prepared.[3,8,9] By contrast, for the (near fcc)[2] Cu-Au system, the average atomic volume increases by about 30% in going from pure Cu to pure Au[4,10] and the alloys may be prepared in both highly ordered and in strongly disordered phases.[5–7]

In an earlier paper[11] we reported a study of dilute alloys of Au dissolved in Cu, Ag, Pd, or Pt in which we investigated a correlation between the charge density at the gold nuclei $\langle|\psi_{Au}(0)|^2\rangle \equiv \rho_{alloy}(0)$ and the residual electrical resistivity due to the gold impurity in the alloy. Here we describe a study of $\rho_{alloy}(0)$ for concentrated alloys of gold. The earlier work was a study of the charge density within

an impurity. The present work may be characterized, in part, as a study of the effect of an impurity on the charge density distribution surrounding it in the host metal.

In previous publications we have also described studies of $\rho_{\text{alloy}}(0)$ as a function of compression[12] for pure gold and for Au_2Mn.[13] Here we describe a similar high-pressure measurement of the volume dependence of $\rho_{\text{alloy}}(0)$ for ordered Cu_3Au. This high-pressure result is useful in the interpretation of our present Au alloy measurements through the theoretical model mentioned above.

There has been extensive interest in the experimental and theoretical study of both the Cu-Au and the Ag-Au alloy systems for a number of years. For the Cu-Au system much information is available about the order dependence of many alloy properties because spatially ordered or disordered phases may be conveniently prepared through suitable heat treatment.[2,14-16] In particular, the electrical resistivity has been found to have a marked order dependence.[2] For example, the resistivities of Cu_3Au and CuAu have been found to change by large factors between ordered and disordered states. This large change of electrical resistance with order implies a corresponding change of the conduction-electron wave function and thus of the charge density distribution which is the subject of this work. These earlier investigations provide an essential basis for our present study.

Previous investigations of charge density distributions in dilute alloys have been made through NMR measurements[17-23] and in concentrated alloys through the use of x-ray scattering techniques.[6,24-26] Mössbauer isomer-shift measurements[27-29] have been used here to study the electron charge density in concentrated alloys because the method is particularly sensitive to small charge density changes and because it probes the alloy charge density over the complete range of concentrations in a direct and distinctive way.

The Mössbauer isomer shift ΔE is the change in the energy of the resonance γ ray of a nucleus associated with a change in chemical environment or state of spatial order. It is related to the average electron charge density at the Mössbauer nuclei (in our case, ^{197}Au) by

$$\Delta E = Kn\,[\rho_{\text{alloy}}(0) - \rho_{\text{Au}}(0)]\,. \tag{1}$$

Here K is a calculable constant,[28] n is a parameter which depends only on nuclear parameters,[28] and $\rho_{\text{alloy}}(0)$ and $\rho_{\text{Au}}(0)$ are the average electron charge densities at gold nuclei in the alloy and for pure gold. In previous studies[11,12] we have given a value for the constant $Kn\rho_{\text{Au}}(0)$ of ~ 8 mm/sec. Other related Mössbauer studies for ^{197}Au are given in Refs. 30-38.

Alloy preparation and some details of the measurements are described in Sec. II, and in Sec. III the results of the measurements are described. In Sec. IV a theoretical model for ΔE is given. In Sec. V, ΔE measurements for Ag-Au, for ordered Cu-Au alloys, and high-pressure measurements for ordered Cu_3Au are discussed in terms of this model.

Preliminary reports of our work on the Cu-Au system have been presented previously.[39,40]

II. MEASUREMENT PROCEDURE AND ALLOY PREPARATION

A. Mössbauer Measurements

The gold Mössbauer measurements reported here were made at 4.2 °K using a sine-wave electromechanical transducer. Data were collected in a multichannel analyzer operating in a pulse-height mode. Sources of the ^{197}Au γ rays were prepared by neutron activation of platinum metal (enriched to 55% ^{196}Pt) in the Oak Ridge National Laboratory research reactor. ^{197}Pt is formed upon the capture of a neutron by ^{196}Pt. The ^{197}Pt decays with a 20-h half-life through the 77.345-keV ($\frac{1}{2}^+$) first excited state of ^{197}Au. The transition from this state to the ($\frac{3}{2}^+$) ground state provided the γ rays used in these experiments. Typical source strengths including all γ rays were about 1 Ci at the beginning of an experiment. The velocity scale was calibrated for each gold Mössbauer spectrum by simultaneously measuring a comparison six-line ^{57}Fe spectrum for an Armco iron absorber[41] at (296 ± 3) °K.

The result of a measurement of the gold Mössbauer absorption line for ordered Cu_3Au at 4.2 °K is shown in Fig. 1. These data are typical of all of the gold measurements to be presented with respect to the number of measured points, their errors, and in the quality of the fit of a theoretical line shape to the data.

The Mössbauer spectra for these nonmagnetic alloys were described by the spin Hamiltonians $\tilde{H}^*$ for the first excited state and $\tilde{H}$ for the ground state, where

$$\tilde{H}^* = \Delta E\,, \tag{2a}$$

$$\tilde{H} = \tfrac{1}{2}p\,[\tilde{I}_z^2 - \tfrac{1}{3}I(I+1)]\,. \tag{2b}$$

In Eq. (2a), ΔE is the isomer shift as defined by Eq. (1). As we have mentioned and as will be described further in Sec. IV the charge density and thus the isomer shift at individual gold sites is expected to depend upon the local configurations of neighboring copper and gold atoms. ΔE of Eq. (1) will thus correspond to an average atomic configuration.

There will be a line broadening which also will reflect the distribution of the possible neighbor configurations in the alloy. For the empirical de-

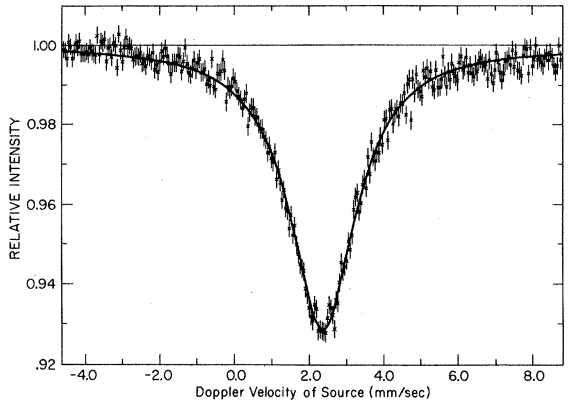

FIG. 1. ^{197}Au Mössbauer absorption line for a 2.13-mil-thick sample of ordered Cu_3Au at 4.2 °K relative to a Au in Pt source. The solid curve is the result of a least-squares fit of a Lorentz line-shape function to the measured points. This result is typical of measurements described in this paper. The error in the isomer-shift measurements is typically ~ 0.01 mm/sec.

scription of the total line broadening we have used a nuclear quadrupole coupling operator $\tilde{H}$ [Eq. (2b)] for the ground state. In this equation, $\tilde{I}_z$ is the z component of the nuclear-spin operator. The constant p will reflect the distribution of atomic configurations through both the electric monopole and quadrupole interactions. There will also be a small contribution to p from sample thickness. This description is possible because p is small compared to our thin sample linewidth. This assumed form for $\tilde{H}$ is found to give a good description of our Mössbauer spectra.

The solid curve in Fig. 1 is a least-squares fit of Eqs. (2a) and (2b) to the experimental data. This fit was obtained using a computer code developed by Czjzek of the Oak Ridge National Laboratory. The code computes an error for the parameters ΔE and p which reflects both the statistical errors in the data points and also the quality of the fit.[42] This is the error which is quoted with the results. In this fit to the data of Fig. 1, the natural linewidth used was $2\Gamma = (1.846 \pm 0.012)$ mm/sec.[43] The p was found to be zero within error, and the isomer shift for this measurement was $\Delta E = (3.527 \pm 0.009)$ mm/sec relative to gold. This error of ~ 0.01 mm/sec is typical of our measurements. On the basis of our result for $Kn\rho_{Au}(0) \sim 8$ mm/sec and from Eq. (1), this error in ΔE corresponds to an error in the measurement of $\rho_{alloy}(0)$ of $10^{-3}\ \rho_{Au}(0)$.

B. Preparation of Ordered and Disordered Alloys

The gold absorber alloys were prepared in a standard foil form so that electrical resistivity and Mössbauer transmission measurements could be made for each sample on the same sample area. For each foil all dimensions were measured to and were uniform to at least 1%. The absorber alloys were produced by the arc melting in an argon atmosphere of high-purity (99.99%) Cu, Au, and Ag metals. The constituents of each alloy were melted and cooled many times and then drop cast (poured) into a water-cooled cylindrical mold. The alloy cylinders were annealed in an inert atmosphere for 5 days within 50 °C of their melting points. From the annealed cylinders, strips were cut lengthwise and then rolled to a thickness of 2 mil with intermittent annealing. Compositions of several of the alloys were checked by chemical analysis by Johnson Matthey Chemicals Limited and were found to agree with our values within $\frac{1}{2}$ at.%.

The alloy foils were ordered by extended heating in a flowing argon atmosphere. The alloys were first subjected to a 100-h anneal at 368 °C and then allowed to furnace cool to 250 °C. This temperature was maintained for 120 h after which the samples were quenched into water at room temperature. The technique described here corresponds to that used by Feder, Mooney, and Nowick.[14] Their lattice parameter measurements[14] indicate that the length of these heat treatments was sufficient to establish equilibrium order at 250 °C. In each case the alloy state of long-range order was checked by a comparison of our resistivity measurements with those of Johansson and Linde (see Fig. 2). Alloy foils were put into a disordered state by a vacuum-quench technique. Each foil was suspended in a vertical vacuum furnace at the quench temperature T_Q for at least 30 min. The sample (with a weight to ensure fast immersion) was then dropped *in vacuo* into a bath of vacuum-pump oil at room temperature. After these heat treatments, the Mössbauer isomer shift of the ^{197}Au nuclei was measured on the central portion of the foils at 4.2 °K. Resistivity measurements were made on the same samples at 296, 78, and 4.2 °K.

C. Short-Range Order of the Alloys

Heat treatments of the above type have been widely used to produce ordered or disordered local atomic environments for the alloy gold atoms. Extensive literature is available[2,4–16,26,44,45] for the Cu-Au and Ag-Au alloy systems which correlates heat treatment procedures and the degree of local atomic order obtained. This order may be described[5] by the short-range-order parameters α_i through the relation

$$\langle n_x \rangle_i = m_x c_i (1 - \alpha_i) . \tag{3a}$$

Here $\langle n_x \rangle_i$ is the average number of x atoms in the ith shell of neighbors about a central gold atom (for a Au-x alloy), m_x is the atomic fraction of x atoms in the alloy, and c_i is the total number of atoms in the ith shell of neighbors. The α_i describe the de-

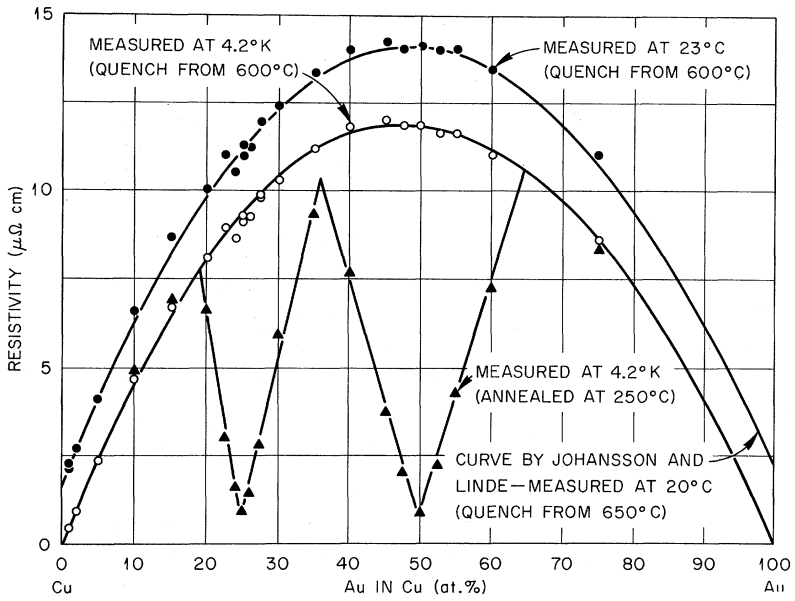

FIG. 2. Electrical resistivity for Cu-Au alloys as a function of composition, and state of order at 4.2 °K, and also for disordered alloys at 296 °K.

viation from total randomness, and $\alpha_i = 0$ corresponds to a completely random alloy.

No measurements of α_i have been made for ordered Cu-Au alloys as a function of composition. Cowley, however, has described[5] a technique for calculating values of α_i as a function of composition for alloys which contain a maximum degree of long-range order. Values of the α_i, determined from this calculation, may give a useful approximation of the actual values of α_i which are obtained from the above extended anneal and quench from 250 °C. Values of α_i for the ordered alloys, calculated through the use of the Cowley model, are given in Table I. The calculation is briefly described below.

Long-range order exists in an alloy if the value of the parameter α_i does not approach zero, but approaches a finite limiting value as i becomes very large. Bragg and Williams[44] have described the long-range order through a parameter S which varies between 0 and 1 and which indicates to what degree the average lattice sites of an alloy are occupied by the correct atoms. The relations between the limiting value of the short-range-order parameter α_i and the long-range-order parameter S depend on the nature of the ordered structure and the composition of the alloy. Cowley[5] has given an expression for the limiting values of α_i for the Cu_3Au-type lattice structure in terms of S as

$$\left.\begin{aligned}\alpha_{i\,\text{even}} &= 3S^2/16 m_{Au} m_{Cu} \\ \alpha_{i\,\text{odd}} &= S^2/16 m_{Au} m_{Cu}\end{aligned}\right\} \text{ } Cu_3Au \text{ structure.} \quad (3b)$$

(Note that Cowley[5] defines a long-range-order parameter S_{Cowley}, which is related to the Bragg-Williams long-range-order parameter S, by $S_{\text{Cowley}} = 3S/16 m_{Au} m_{Cu}$ for Cu_3Au alloys and $S_{\text{Cowley}} = S/4 \times m_{Au} m_{Cu}$ for CuAu alloys.) For a layered but nearly fcc-type lattice structure (the approximate configuration for alloys with compositions near CuAu)

TABLE I. Approximate short-range-order parameters and relative atomic volumes.

Alloy	Limiting values ($T=0$)[a] α_1	α_2	Relative atomic volume[b] (v_{Au}/v)
Alloys with a maximum degree of long-range order			
Cu	0	0	1.4377
$Au_{05}Cu_{95}$	−0.053	0.159	1.4052
$Au_{10}Cu_{90}$	−0.111	0.333	1.3739
$Au_{15}Cu_{85}$	−0.176	0.529	1.3434
$Au_{20}Cu_{80}$	−0.250	0.750	1.3139
$Au_{25}Cu_{75}$	−0.333	1.000	1.2835
$Au_{30}Cu_{70}$	−0.259	0.778	1.2578
$Au_{35}Cu_{65}$	−0.206	0.619	1.2328
$Au_{40}Cu_{60}$	−0.222	0.667	1.2085
$Au_{45}Cu_{55}$	−0.273	0.818	1.1878
$Au_{50}Cu_{50}$	−0.333	1.000	1.1677
$Au_{55}Cu_{45}$	−0.273	0.818	1.1479
$Au_{60}Cu_{40}$	−0.222	0.667	1.1288
$Au_{65}Cu_{35}$	−0.179	0.538	1.1103
$Au_{70}Cu_{30}$	−0.143	0.429	1.0923
$Au_{75}Cu_{25}$	−0.111	0.333	1.0742
$Au_{80}Cu_{20}$	−0.083	0.250	1.0567
$Au_{85}Cu_{15}$	−0.059	0.176	1.0417
$Au_{90}Cu_{10}$	−0.037	0.111	1.0271
$Au_{95}Cu_{05}$	−0.019	0.053	1.0134
Au	0	0	1.0000
Alloy quenched from temperature T_Q ($T_Q = 800$ °C)			
$Au_{25}Cu_{75}$	−0.273	0.450	1.2826

[a]Reference 5.
[b]Reference 4.

the Cowley model may again be used to express the limiting values of α_i as a function of the Bragg-Williams long-range-order parameter S as

$$\left.\begin{aligned}\alpha_{i\ \text{even}} &= S^2/4m_{\text{Au}}m_{\text{Cu}} \\ \alpha_{i\ \text{odd}} &= -S^2/12m_{\text{Au}}m_{\text{Cu}}\end{aligned}\right\}\ \text{Cu Au structure.} \qquad (3c)$$

In this approximate calculation the effects of lattice distortion and antiphase domain boundaries found[2] for CuAu are neglected.

The maximum value for the Bragg-Williams long-range-order parameter S_{max} (corresponding to the maximum degree of long-range order in an alloy) is a function of the composition of the alloy. Krivoglaz[46] has given this maximum value as

$$\left.\begin{aligned}S_{\text{max}} &= 4m_{\text{Cu}} \quad \text{for } 0 \le m_{\text{Cu}} \le 0.25 \\ S_{\text{max}} &= \tfrac{4}{3}m_{\text{Au}} \quad \text{for } 0.25 \le m_{\text{Cu}} \le 0.37\end{aligned}\right\}\ \text{Cu}_3\text{Au structure},$$

$$\left.\begin{aligned}S_{\text{max}} &= 2m_{\text{Cu}} \quad \text{for } 0.37 < m_{\text{Cu}} \le 0.50 \\ S_{\text{max}} &= 2m_{\text{Au}} \quad \text{for } 0.50 \le m_{\text{Cu}} \le 1.00\end{aligned}\right\}\ \text{CuAu structure.} \qquad (3d)$$

These values for S_{max} have been checked experimentally for the Cu_3Au-type alloys ($m_{\text{Cu}} = 0.20$, 0.23, 0.28, 0.30, and 0.34) by Jaumot and Sutcliffe[15] using x-ray diffraction and are found to agree with experiment within error.

Equations (3b)–(3d) describe the limiting values of the short-range-order parameter α_i, as a function of composition, for those alloys which have a maximum degree of long-range order. For the Cu-Au alloy system, the phase diagram[3,47] suggests that for low temperatures the Cu_3Au-type lattice exists for compositions in the range $0 \le m_{\text{Au}} \le \sim 0.37$ and that the CuAu-I–type lattice exists for composition in the range $\sim 0.37 < m_{\text{Au}} \le 1.00$. Breaking the total composition range into four subranges and using Eqs. (3b)–(3d), we thus arrive at the following expressions in Eqs. (3e) for the limiting values of α_i in the ordered Cu-Au alloys:

$$\begin{aligned}\alpha_0 &= -\tfrac{1}{3}\alpha_e = -m_{\text{Au}}/m_{\text{Cu}} \quad \text{for } 0 \le m_{\text{Au}} \le 0.25, \\ \alpha_0 &= -\tfrac{1}{3}\alpha_e = -m_{\text{Cu}}/9m_{\text{Au}} \quad \text{for } 0.25 \le m_{\text{Au}} \le 0.37, \\ \alpha_0 &= -\tfrac{1}{3}\alpha_e = -m_{\text{Au}}/3m_{\text{Cu}} \quad \text{for } 0.37 < m_{\text{Au}} \le 0.50, \\ \alpha_0 &= -\tfrac{1}{3}\alpha_e = -m_{\text{Cu}}/3m_{\text{Au}} \quad \text{for } 0.50 \le m_{\text{Au}} \le 1.0.\end{aligned} \qquad (3e)$$

Here α_0 describes all shells of neighbors for which the index i is an odd integer, and α_e all shells for which i is even. At low temperatures, and for an alloy which has a maximum degree of long-range order, we shall take $\alpha_1 = \alpha_0$ and $\alpha_2 = \alpha_e$. These are the values given in Table I.

The order parameters for the infinitely dilute alloys are exact. This is also the case for Cu_3Au and CuAu in so far as they have complete long-range order. The order parameters which are given in Table I are thus expected to be good approximations near these compositions.

In the case of disordered alloys, many experimental and theoretical studies have been made to determine equilibrium values of α_i for Cu-Au alloys at temperatures above the critical long-range-order transition temperature T_c. These high-temperature values of α_i are not expected to be "frozen in" by even a fast quench to room temperature. The resistivity measurements of Schule,[48] the x-ray measurements of Borie and Warren,[26] and the heat-release measurements of Hirabayaski *et al.*[49] indicate that the α_i for Cu_3Au change from their equilibrium values at high temperatures during the quenching process to room temperature. For the disordered systems, the only available value of α_i relevant to our measurements is for Cu_3Au. This value was obtained by Moss[7] from room-temperature measurements on a sample disordered at a temperature of 800 °C and quenched to room temperature. This room-temperature value, which is also given in Table I, is assumed to apply at 4.2 °K where our isomer-shift measurements were made.

III. MÖSSBAUER ISOMER-SHIFT AND ELECTRICAL RESISTIVITY MEASUREMENTS

A. Isomer-Shift Measurements as a Function of Composition and Order for Cu-Au Alloys

In Fig. 3 we give the results of the isomer-shift measurements for the ordered and disordered phases of the 23 Cu-Au alloy compositions studied. The ΔE measurements were made at 4.2 °K. In this figure the isomer shift is given relative to gold. The straight line shown connects the pure-gold isomer shift with the extrapolated value of (4.049 ± 0.005) mm/sec for an infinitely dilute solution of Au in Cu. For this case of an infinitely dilute solution of Au in Cu and on the basis of our result for $Kn\rho_{\text{Au}}(0) \sim 8$ mm/sec, the fractional change of charge density $[\rho_{\text{alloy}}(0) - \rho_{\text{Au}}(0)]/\rho_{\text{Au}}(0) \sim 0.5$. Thus, in going from pure gold to the infinitely dilute solution the charge density at the gold nucleus due to the conduction electrons increases by ~50%.

In Fig. 3 the open circles give ΔE for the ordered alloys (annealed at 250 °C) and the solid circles correspond to the "disordered alloys" (quenched from 600 °C). The errors in the measurements of ΔE (~0.01 mm/sec) are much smaller than would be indicated by the size of the plotted points. The isomer shifts for the ordered and disordered phases are close together in value below ~10% and above ~70% gold in copper. The difference between the isomer shifts for the two types of heat treatments (degrees of order) is largest near the compositions Cu_3Au and CuAu. For all compositions, the more highly ordered phase is found to have the more positive isomer shift within experimental error. From Eq. (1), this corresponds to a greater electron

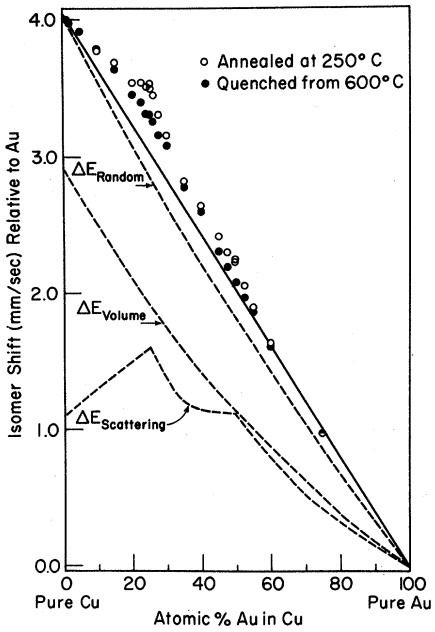

FIG. 3. Mössbauer isomer shift for ^{197}Au as a function of composition and state of order for Cu-Au alloys. Measured points for ordered alloys (annealed at 250 °C) are open circles. Solid circles are the measured isomer-shift values for disordered alloys (quenched from 600 °C). The isomer shift, and thus $|\psi(0)|^2$, is greater for the more highly ordered state. The solid straight line is used as a reference for the data which are replotted in Fig. 4. Through the use of an approximate model for the isomer shift, Secs. IV and V, an estimate of the isomer shift which would be expected for a totally random alloy was made. This estimate ΔE_{Random} is considerably below the observed isomer shift for the disordered alloys. This indicates that a substantial degree of short-range order remains in these disordered samples. Using this same model, estimates have been made of the effects of alloy atomic volume ΔE_{volume} and of scattering $\Delta E_{\text{scattering}}$ on the alloy isomer shift. ΔE_{volume} is larger than $\Delta E_{\text{scattering}}$ for Cu-Au alloys.

charge density[11,12,31,38] at the gold nuclei for the more highly ordered state.

In order to more easily see the detailed behavior of ΔE with composition and heat treatment, the straight line of Fig. 3 has been subtracted from all the data points. This difference $\delta(\Delta E)$ is plotted in Fig. 4. The solid line in this figure is the prediction of a model for ΔE [or $\rho_{\text{alloy}}(0)$] given in Secs. IV and V. From Fig. 4 we see that the change of ΔE between the ordered and disordered phases for Cu_3Au and CuAu is about 0.2 mm/sec. Taking $Kn\rho_{\text{Au}}(0) = 8$ mm/sec, this decrease of ΔE corresponds to a fractional decrease of charge density $\Delta\rho_{\text{alloy}}(0)/\rho_{\text{Au}}(0)$ of 0.025.

As has been shown by Clapp and Moss,[6] and as we have discussed above, the heat treatments which we have used can produce highly ordered alloys but yield quenched alloys which are only partially disordered. It is expected that the change of ΔE and of $\rho_{\text{alloy}}(0)$ between perfect order and total randomness would be larger than the changes we have observed. An estimate given in Sec. V of ΔE for total randomness is shown in Fig. 3 as ΔE_{random}.

B. Isomer Shift for Cu_3Au as a Function of Quench Temperature

In Fig. 5, the measured values of the Mössbauer isomer shift are given for Cu_3Au as a function of quench temperature T_Q for T_Q both above and below the critical long-range-ordering temperature T_c. With increasing T_Q a sharp decrease of ΔE is observed at T_c. As noted above, this behavior corresponds to a decrease of $\rho_{\text{alloy}}(0)$ at the critical temperature. The dotted curve is an interpolation between the measured points. The fractional change in ΔE observed in Fig. 5 is relatively small in contrast with that of the electrical resistivity in Fig. 2 which changes by a large factor with T_Q as T_Q goes through T_c. The point × in Fig. 5 is a prediction of a model for ΔE [or $\rho_{\text{alloy}}(0)$] given in Secs. IV and V.

C. Isomer Shift for Ag-Au Alloys

In the case of the Ag-Au alloy system previous work has indicated[8] that the 250 °C heat treatment used for the Cu-Au alloys does not lead to appreciable spatial order. It was thus of interest to measure ΔE for 1% Au in Ag, Ag_3Au, and AgAu after (a) an anneal at 250 °C for 120 h and then (b) after a quench from 600 °C. The values for ΔE for these measurements are given in Fig. 6. It may be seen that within experimental error ΔE is independent of these heat treatments and also that ΔE is linearly dependent on composition. The significance of this linear dependence will be discussed in Sec. V.

D. Measurement of Isomer Shift for Ordered Cu_3Au at 65 kbars

A measurement of ΔE has been made for ordered Cu_3Au at 4.2 °K and at applied pressures P of 0 and of 65 kbar. The equipment and procedures used for this measurement have been described previously.[12] The change of metallic volume $\Delta v/v_0$ as a function of P may be discribed by

$$\Delta v/v_0 = aP + bP^2 ,$$

where $a = 3/(c_{11} + 2c_{12})$, and in a model suggested by Slater,[50] $b \cong 3a^2$. Flinn[51] has measured these elastic constants at 4.2 °K and has given the values $c_{11} = (1.893 \pm 0.015) \times 10^{12}$ dyn/cm^2 and $c_{12} = (1.319 \pm 0.015) \times 10^{12}$ dyn/cm^2. The results from these measurements along with some results taken from a more extensive study for metallic gold are given in Table II, and discussed in Sec. V.

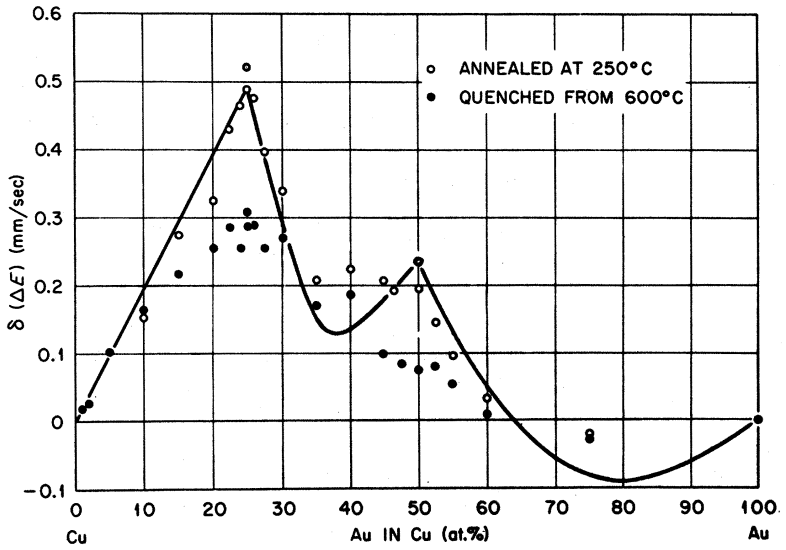

FIG. 4. The reference straight line of Fig. 3 has been subtracted from the data points and this isomer-shift increment $\delta\Delta E$ has been plotted here on an expanded scale. The solid line shows a fit of the theoretical model for the isomer shift given in Secs. IV and V to the data for the ordered alloys.

E. Mössbauer Linewidth

As we have discussed in Sec. II, the linewidth for the alloys has been discribed empirically through a quadrupole coupling operator Eq. (2b). In Fig. 7 the empirical width parameter p is plotted for both the ordered and disordered alloys. For Cu_3Au, p is zero within experimental error, and near Cu_3Au, p is smaller for the ordered than for the disordered state. In the region of the layered CuAu structure, p is large and changes only by a small amount with the degree of order, and is less for the disordered state.

Thus far we have made only a preliminary theoretical study of the experimental line shape. For the case of disordered Cu_3Au a distribution of the local atomic configurations has been calculated for an assumed random alloy. Using the model for ΔE in Eq. (18) of Sec. IV and this distribution of atomic configurations in Eq. (18), the line shape has been calculated and compared with the experimental line shape. This procedure gave a remarkably good fit to the experimental data. The result is somewhat accidental, however, for we do not expect the actual alloy to be totally disordered. The above calculation for a random alloy probably gives an overestimate of the contribution of the monopole interaction to the linewidth. As we have discussed above, quadrupole coupling effects will be expected to contribute to this linewidth also. To calculate the line shapes for the concentrated alloys we will require detailed information about the distribution of neighbor configurations. We have not undertaken this calculation.

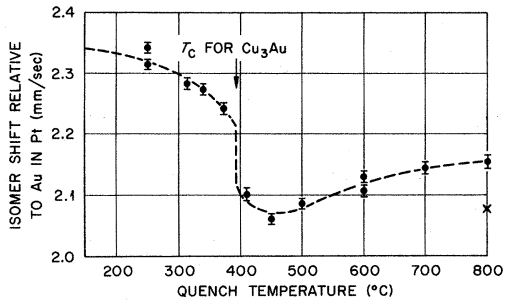

FIG. 5. Gold Mössbauer isomer shift for Cu_3Au as a function of quench temperature T_Q. The dotted curve is suggested pictorial interpolation through the experimental points. It does not represent any theoretical model. A rapid change of isomer shift with T_Q is observed near the critical long-range-ordering temperature $T_c = 395\,°C$. Point x was calculated from the model for the isomer shift given in Secs. IV and V using order parameters measured by Moss for the quenched sample (see Table I).

F. Electrical Resistivity of Cu-Au and Ag-Au Alloys

In addition to the above measurements of ΔE, we have measured the electrical resistivity of the Mössbauer alloy sample for each composition and heat treatment. Care was taken to make these resistivity measurements for the same area of the sample foils as that through which the Mössbauer γ

TABLE II. Mössbauer isomer-shift measurements at 4.2 °K for gold and ordered Cu_3Au at 0 and 65 kbar.

Metal	Pressure (kbar)	(v_{Au}/v)	ΔE (mm/sec) Relative to Au in Pt
Au	0	1.000	-1.220 ± 0.005
Au	65	1.034	-0.990 ± 0.020
Cu_3Au	0	1.284	2.311 ± 0.016
Cu_3Au	65	1.341	2.626 ± 0.027

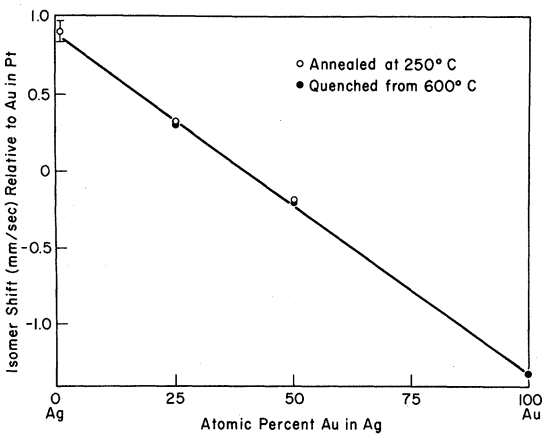

FIG. 6. Isomer shift for ^{197}Au in Ag-Au alloys as a function of composition and heat treatment. A linear dependence of the isomer shift on composition is predicted by the theoretical model of Secs. IV and V.

rays were passed. The resistivity measurements were made at 4.2, 77, and at 296 °K. The results of some of these measurements are given above in Fig. 2. Measurements of this type were first made by Johansson and Linde[2] at 293 °K. Our room-temperature measurements agree very well with their work. As far as we are aware, resistivity studies at 4.2 °K over the complete range of composition and order have not been reported previously.

The electrical resistivity of Cu_3Au as a function of quench temperature T_Q for $T_Q < T_c$ is given in Fig. 8. These measurements were made at 4.2, 77, and 296 °K. The 23 °C measurements show a minimum in the resistivity for T_Q near 450 °C. Above T_c the isomer shift and the resistivity are seen to have a similar dependence on T_Q.

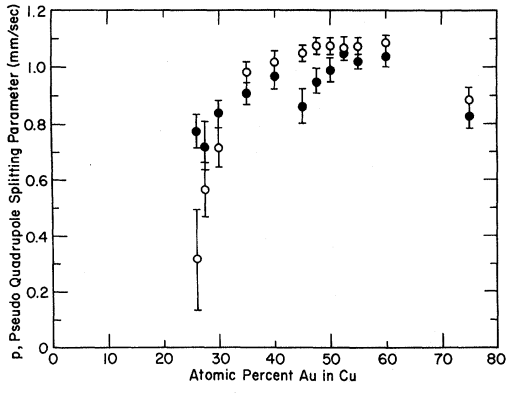

FIG. 7. The Mössbauer line broadening for thin samples is described approximately as a pseudoquadrupole coupling. Measured values of the coupling parameter p are given here as a function of composition for ordered and disordered Cu-Au alloys.

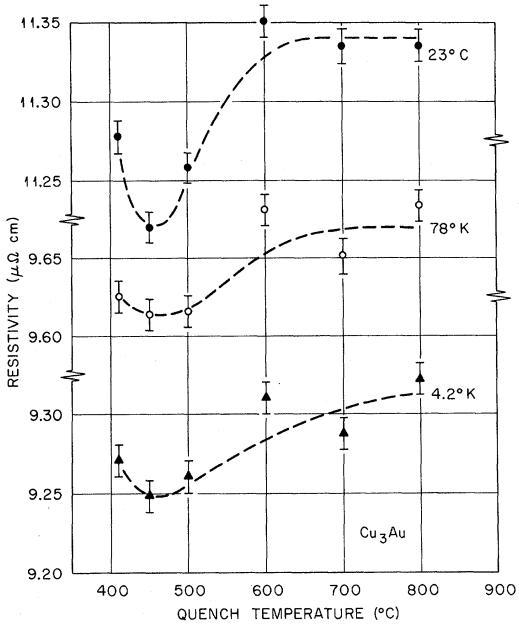

FIG. 8. Electrical resistivity in $\mu\Omega$ cm for Cu_3Au as a function of quench temperature T_Q (°C). Resistivity measurements were made at 4.2, 78, and 296 °K. The resistivity is lower for lower T_Q. Dotted curves are a suggested pictorial interpolation between the points.

Values of the electrical resistivity for AgAu and Ag_3Au after a quench from 600 °C and after an anneal at 250 °C have also been determined at 4.2, 77, and 296 °K. These results, given in Table III, show no change of resistivity with heat treatment.

These resistivity measurements are helpful in giving assurance that our samples have the expected compostion and degree of order. They will be useful also in obtaining parameters for a pseudopotential treatment of these isomer-shift measurements.[11,52,53]

IV. A THEORETICAL MODEL FOR THE ISOMER SHIFT FOR THE CUBIC BINARY ALLOYS

In this section, we describe an approximate theoretical model for the isomer shift ΔE which gives an explicit dependence of ΔE on alloy composition, average atomic volume, and on short-range order. In order to indicate the nature of the approximations which will be made we will begin with a wave function which is exact in a single-electron description, and trace the development of the model which we compare with our measurements in Sec. V.

The normalized wave function for an electron at a point $\vec{r}$ in the alloy and with a state index $\vec{k}$, $\psi_{\text{alloy},\vec{k}}(\vec{r})$, may be written as a superposition of an incident wave $\psi_{a,\vec{k}}(\vec{r})$ and of waves scattered from potentials located at atomic sites j, $\psi_{s,\vec{k},j}(\vec{r}-\vec{r}_j)$,

$$\psi_{\text{alloy},\vec{k}}(\vec{r}) = \psi_{a,\vec{k}}(\vec{r}) + \sum_j \psi_{s,\vec{k},j}(\vec{r}-\vec{r}_j) \,. \qquad (4)$$

$\vec{r}_j$ gives the position of the nucleus of the jth atom. If we neglect small product terms of the form $\psi^*_{s,\vec{k},j}(\vec{r}-\vec{r}_j)\psi_{s,\vec{k},j'}(\vec{r}-\vec{r}_{j'})$ due to the scattered waves from potentials located at $\vec{r}_j$ and $\vec{r}_{j'}(j \neq j')$, the probability density at a point $\vec{r}$ in the alloy may be written as a sum of densities

$$\rho_{\text{alloy}}(\vec{r}) = \rho_a(\vec{r}) + \sum_j \rho_j(\vec{r}-\vec{r}_j) \ . \tag{5}$$

Here,

$$\rho_{\text{alloy}}(\vec{r}) = \int_F n(\vec{k}) \left| \psi_{\text{alloy},\vec{k}}(\vec{r}) \right|^2 d^3k \ , \tag{6a}$$

$$\rho_a(\vec{r}) = \int_F n(\vec{k}) \left| \psi_{a,\vec{k}}(\vec{r}) \right|^2 d^3k \ , \tag{6b}$$

$$\rho_j(\vec{r}-\vec{r}_j) = \int_F n(\vec{k}) [2 \left| \psi^*_{a,\vec{k}}(\vec{r}) \psi_{s,\vec{k},j}(\vec{r}-\vec{r}_j) \right| + \left| \psi_{s,\vec{k},j}(\vec{r}-\vec{r}_j) \right|^2] d^3k, \tag{6c}$$

where $n(\vec{k})$ is the density of states and the integrals are over the volume F of occupied states in $\vec{k}$ space. The density term neglected above is expected to be small compared to $\rho_j(\vec{r}-\vec{r}_j)$, as will be discussed in Sec. V.

When choosing a convenient form for the incident wave $\psi_{a,\vec{k}}(\vec{r})$, it is useful to consider the spatial configuration of atomic positions in the alloy. For a binary solid solution where the component metal atoms have different radii, the atoms will, in general, fall at positions which are at small random displacements from the sites of a reference or average lattice that has translational symmetry. For an alloy of Au with a metal x, the position vectors $\vec{r}_j$ and $\vec{r}_l$ will denote Au and x nuclear positions. We now consider a hypothetical sample of pure but distorted metallic gold which is prepared by replacing all x atoms at the $\vec{r}_l$ sites by Au atoms. In this replacement the spatial configuration of nuclear positions of the alloy, defined by the set of $\vec{r}_j$ and $\vec{r}_l$, is to remain unchanged. We shall further suppose that the quantum-mechanical problem for this distorted configuration of gold atoms has been solved and that the wave functions for the valence band, or continuum of states, has been obtained. We take an incident wave, $\psi_{a,\vec{k}}(\vec{r})$ of Eqs. (4) and (6b), to be one of these eigenstates for distorted metallic gold.

For the actual alloy, the potential associated with a gold site $\vec{r}_j$ is expected to be similar and close in magnitude to the potential found at that same site in the distorted gold metal. On the other hand, the potential associated with an x atom site $\vec{r}_l$ in the alloy will, in general, be quite different from the potential at that site in the distorted gold. Thus in the theoretical description of the alloy, $\psi_{a,\vec{k}}(\vec{r})$ will be scattered at both gold and x atomic sites, but the scattered charge density $\rho_{\text{Au}}(\vec{r}-\vec{r}_j)$ [Eq. (6c)] associated with scattering at gold sites is expected to be less in magnitude than the $\rho_x(\vec{r}-\vec{r}_l)$ associated with x sites.

From Eq. (5), the probability density at some specific gold nucleus located at $\vec{r}_{\text{Au}}$ in an alloy of Au with metal x is

$$\rho_{\text{alloy}}(\vec{r}_{\text{Au}}) = \rho_a(\vec{r}_{\text{Au}}) + \sum_j \rho_{\text{Au}}(\vec{r}_{\text{Au}}-\vec{r}_j) + \sum_l \rho_x(\vec{r}_{\text{Au}}-\vec{r}_l) \ . \tag{7}$$

In Mössbauer measurements the isomer shift depends on the average electron charge density at the gold nuclei in the alloy $\rho_{\text{alloy}}(0)$. Thus

$$\rho_{\text{alloy}}(0) = N_{\text{Au}}^{-1} \sum_{\substack{\text{Au} \\ \text{sites}}} \rho_{\text{alloy}}(\vec{r}_{\text{Au}}) \ , \tag{8}$$

where N_{Au} is the number of gold atoms in the sample. This may be written in the form

$$\rho_{\text{alloy}}(0) = \bar{\rho}_a(0) + \sum_i [\langle n_{\text{Au}} \rangle_i \bar{\rho}_{\text{Au}}(r_i) + \langle n_x \rangle_i \bar{\rho}_x(r_i)] \ . \tag{9}$$

Here

$$\bar{\rho}_a(0) = N_{\text{Au}}^{-1} \sum_{\substack{\text{Au} \\ \text{sites}}} \rho_a(\vec{r}_{\text{Au}}) \ , \tag{10a}$$

$$\bar{\rho}_{\text{Au}}(r_i) = N_{\text{Au},i}^{-1} \sum_{\substack{\text{Au} \\ \text{sites}}} \sum_{j=1}{}' \rho_{\text{Au}}(\vec{r}_{\text{Au}}-\vec{r}_j) \ , \tag{10b}$$

$$\bar{\rho}_x(r_i) = N_{x,i}^{-1} \sum_{\substack{\text{Au} \\ \text{sites}}} \sum_{l=i}{}' \rho_x(\vec{r}_{\text{Au}}-\vec{r}_l) \ , \tag{10c}$$

$$N_{\text{Au},i} = \sum_{\substack{\text{Au} \\ \text{sites}}} n_{\text{Au},i} = N_{\text{Au}} \langle n_{\text{Au}} \rangle_i \ , \tag{10d}$$

and

$$N_{x,i} = \sum_{\substack{\text{Au} \\ \text{sites}}} n_{x,i} = N_{\text{Au}} \langle n_x \rangle_i \ . \tag{10e}$$

In Eqs. (10b) and (10c), the $\sum'$ is a sum only over those Au sites $\vec{r}_j$ or those x sites $\vec{r}_l$ which are in the ith shell of neighbors to a gold atom. $\langle n_{\text{Au}} \rangle_i$ and $\langle n_x \rangle_i$ are the average numbers, for the entire

TABLE III. Electrical resistivity of the Ag-Au alloys at 4.2, 77, and 296 °K.

Alloy	Measurement temperature (°K)	Resistivity ($\mu\Omega$ cm) quenched from 250 °C	Resistivity ($\mu\Omega$ cm) quenched from 600 °C
Ag_3Au	4.2	6.73 ± 0.07	6.69 ± 0.07
	77.0	7.10 ± 0.07	7.05 ± 0.07
	296.0	8.62 ± 0.08	8.59 ± 0.08
AgAu	4.2	8.77 ± 0.09	8.75 ± 0.09
	77.0	9.18 ± 0.09	9.17 ± 0.09
	296.0	10.84 ± 0.11	10.86 ± 0.11

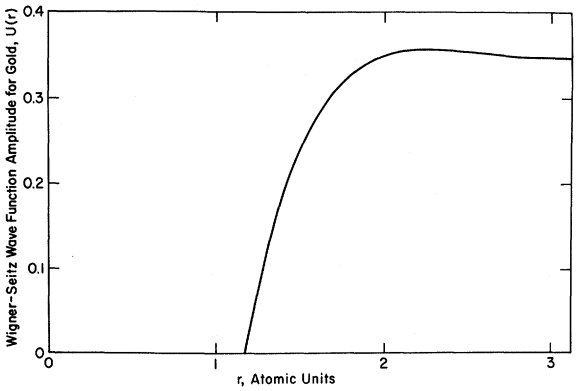

FIG. 9. Large component of DWSS wave function amplitude for the gold $6s_{1/2}$ atomic state beyond the outermost node as a function of radius in a.u. W-S cell radius here is 3.00 a.u. units, the value for pure gold (see Ref. 54).

sample, of gold atoms or of x atoms in an ith shell. For any shell $n_{\mathrm{Au},i}+n_{x,i}=c_i$ (see Sec. IIC). Equations (10d) and (10e) are thus simply related. r_i is the radius of the ith shell in the average lattice of the alloy. The quantities $\overline{\rho}_a(0)$, $\overline{\rho}_x(r_i)$, and $\overline{\rho}_{\mathrm{Au}}(r_i)$ will, in general, depend on alloy composition, state of order, and on the parameters of the average lattice.

Within the single-electron approximation, and apart from the above omission of small interference terms, the above theoretical framework is exact. In order to compare Eq. (9) to our isomer-shift measurements we will make several additional approximations.

As we have mentioned above, in the alloy, $\psi_{a,\vec{k}}(\vec{r})$ will, in general, be scattered at both Au and x sites. At an x site in the alloy the ion potential will be quite different from the potential at this site in the distorted gold and $|\psi_s(\vec{r})|/|\psi_a(\vec{r})|$ may be appreciable though small relative to 1. At a gold site, however, the gold ion potential in the alloy and in the distorted gold may be expected to be more nearly the same and the scattering of $\psi_{a,\vec{k}}(\vec{r})$ at gold sites is expected to be relatively weak. On this basis we assume that $\rho_a(0)\gg\rho_x(r_i)\gg\rho_{\mathrm{Au}}(r_i)$ and we shall neglect the term in $\rho_{\mathrm{Au}}(r_i)$ in Eq. (9). Equation (9) then becomes

$$\rho_{\mathrm{alloy}}(0)=\overline{\rho}_a(0)+\textstyle\sum_i\langle n_x\rangle_i\overline{\rho}_x(r_i)\ . \tag{11}$$

In the following, the incident wave $\psi_{a,\vec{k}}(\vec{r})$, and thus $\rho_a(\vec{r}_{\mathrm{Au}})$ and $\overline{\rho}_a(0)$, will be treated approximately in terms of a Wigner-Seitz (W-S) model. As is illustrated in Fig. 9, the W-S function for gold $U(r)$ is nearly constant in the outer region of the atom. In the range $2\leq r\leq 3$ a.u., $U(r)$ is constant to within $\approx 1\%$ of the value 0.352 for pure mettallic Au. Here, the W-S radius is $R_{\mathrm{Au}}=3.00$ a.u. We shall assume that, for the distorted gold, the $6s$ W-S wave function $U(r)$ surrounding every gold nucleus in the metal is the same for $0\leq r\leq\sim 2$ a.u. and that $U(r)$ is constant in the region between these "cores." The W-S radius for copper is $R_{\mathrm{Cu}}=2.67$ a.u. It is thus reasonable to assume that in the distorted gold (as in the Cu-Au alloys) no internuclear separation will be less than $\sim(R_{\mathrm{Au}}+R_{\mathrm{Cu}})$ or ~ 5.7 a.u. Thus, even in the hypothetical distorted gold, the displacement of the atoms is small relative to the extensive outer region of the atom where $U(r)$ is approximately constant. The incident wave will be taken to have the form

$$\psi_{a,\vec{k}}(\vec{r})=e^{i\vec{k}\cdot\vec{r}}\sum_j\frac{U(\vec{r}-\vec{r}_j)}{\sqrt{V}} \tag{12}$$

within a gold atom at $\vec{r}_j$ in the distorted gold. The V in Eq. (12) is the volume of the alloy sample.

The normalization of $\psi_{a,\vec{k}}(\vec{r})$ is such that one electron of each spin projection may occupy each $\vec{k}$ state. In the distorted gold a W-S cell may be associated with each site $\vec{r}_j$. This cell will be a distorted polyhedron of volume v_j. The normalization of $U(r)$ is taken to be such that

$$v^{-1}\int_v|U(|\vec{r}-\vec{r}_j|)|^2d\tau=1\ , \tag{13a}$$

where $v=\overline{v}_j$ is the average atomic or W-S cell volume in the distorted gold (also in the alloy) and where this spherical W-S cell volume is centered at $\vec{r}_j$.

$$\int_v|\psi_{a,\vec{k}}(\vec{r})|^2d\tau=v/V \tag{13b}$$

and

$$\int_V|\psi_{a,\vec{k}}(\vec{r})|^2d\tau=1\ , \tag{13c}$$

where $v=\overline{v}_j=V/N$ and $N=N_{\mathrm{Au}}+N_x$ is the total number of atoms in the alloy sample. The charge density at all of the gold nuclei in the distorted gold in this model for the incident wave will be the same and

$$\rho_{\mathrm{Au}}(0)=\overline{\rho}_a(0)=U^2(0)N/V\ , \tag{14}$$

where N is the total number of Au and x atoms and N/V is the number of s-band electrons per cubic centimeter in the alloy. For the distorted gold, as for the Cu-Au system, we assume this $N/V=\overline{v}_j^{-1}$ or one $6s$ electron per atom.

The scattered wave $\psi_{s,\vec{k},l}(\vec{r}-\vec{r}_l)$ will also be treated in a W-S approximation. Within a gold atom at $\vec{r}_j$, the contribution to the wave function due to scattering from an atom at $\vec{r}_l$ will be taken to have the form

$$\psi_{s,\vec{k},l}(\vec{r}-\vec{r}_l)=U(\vec{r}-\vec{r}_j)\,\phi_{s,\vec{k},l}(\vec{r}-\vec{r}_l)/\sqrt{V}\ . \tag{15a}$$

Compared with $U(\vec{r}-\vec{r}_j)$, $\phi_{s,\vec{k},l}(\vec{r}-\vec{r}_l)$ is assumed to be a slowly varying function of $\vec{r}-\vec{r}_l$. The alloy wave function within a gold atom at the origin will have the form

$$\psi_{\text{alloy},\vec{k}}(\vec{r}) = [U(\vec{r})/\sqrt{V}]\,[e^{i\vec{k}\cdot\vec{r}} + \textstyle\sum_l \phi_{s,\vec{k},l}(\vec{r}-\vec{r}_l)]\,. \tag{15b}$$

We anticipate that it will be possible to calculate the scattered wave function $\phi_{s,\vec{k},l}(\vec{r}-\vec{r}_l)$ (and hence the scattered charge density) through the use of a pseudopotential model.[11]

Because of the normalization of $\psi_{a,\vec{k}}(\vec{r})$ [Eq. (12)] the wave function for $\psi_{\text{alloy},\vec{k}}(\vec{r})$ [Eq. (15b)] appears to be unnormalized. We assume, however, that $\langle\psi_{\text{alloy},\vec{k}} \mid \psi_{\text{alloy},\vec{k}}\rangle = \langle\psi_{a,\vec{k}} \mid \psi_{a,\vec{k}}\rangle = 1$. This condition would occur if, for example, charge which appeared within a gold atom specifically due to scattering from the x sites was displaced from within the x-atom scattering centers.

Substituting Eq. (15b) into Eq. (6) and Eq. (6) into Eqs. (10), (14), and then (11), the average charge density at the gold nuclei becomes

$$\rho_{\text{alloy}}(0) = [U^2(0)N/V]\,[1 + \textstyle\sum_i \langle n_x\rangle_i \rho_{x,s}(r_i)]\,, \tag{16a}$$

where

$$\bar{\rho}_x(r_i) = [U^2(0)N/V]\,\bar{\rho}_{x,s}(r_i) \tag{16b}$$

and

$$\bar{\rho}_{x,s}(r_i) = N_{x,i}^{-1} \sum_{\substack{\text{Au}\\ \text{sites}}} {\sum_{l=i}}' \int_F n(\vec{k}) \{2 \left| e^{-i\vec{k}\cdot\vec{r}} \phi_{s,\vec{k},l}(\vec{r}-\vec{r}_l)\right| + \left|\phi_{s,\vec{k},l}(\vec{r}-\vec{r}_l)\right|^2\} d^3k\,. \tag{16c}$$

Friedel oscillations as seen by the Mössbauer isomer shift are thus given by this term $\bar{\rho}_{x,s}(r_i)$.

As will be seen in Sec. V, $\bar{\rho}_{x,s}(r_i) \ll 1$ for r_i equal to or greater than a nearest-neighbor distance. We shall assume that $\bar{\rho}_{x,s}(r_i)$ has only a weak dependence on volume and composition. In that the difference of the gold and copper pseudopotentials should have only a weak dependence on these variables, this assumption should be reasonable.

The average electron charge density throughout a pure metal sample is, of course, simply N/V, the number of electrons per cubic centimeter. The electron charge density at the nuclei, however, will, in general, have a volume dependence which differs from v^{-1}. The volume dependence of $U^2(0)N/V$ has been investigated theoretically for Au by Tucker *et al.*[54] in a Dirac-Wigner-Seitz-Slater (DWSS) approximation where Au was assumed to be in a $5d^{10}\,6s$ configuration. In this approximation the charge density at the gold nuclei was found to be closely proportional to $v^{-\gamma}$ for a wide range of volume. γ was found to have a value of 0.86 near the atomic volume of metallic gold. Within these approximations

$$\bar{\rho}_a(0) = U^2(0)N/V = \rho_{\text{Au}}(0)\,(V_{\text{Au}}/V)^{\gamma}\,. \tag{17}$$

In this gold DWSS calculation[54] the $6s$ charge density was found to accumulate preferentially in the outermost region of the atom as the atomic cell was compressed. The core region of the atom resisted penetration of the $6s$ charge. This resistance to penetration is described in Eq. (17) through the fact that $\gamma < 1$. In this W-S model for $\rho_{\text{alloy}}(0)$ the use of a pure $5d^{10}6s$ configuration will give an overestimate of the amount of $6s$ character for gold metal, and may give an overestimate for γ. Anticipating the result of Sec. V D we note that, using the theoretical model given here and within the experimental error in our high-pressure isomer-shift measurements, γ is the same for pure Au and for Cu_3Au; i.e., γ is at least approximately independent of alloy composition. As far as we are aware no measurement of γ has been made. For the present we will take the theoretical DWSS value $\gamma = 0.86$.

Ingalls[55] and Ingalls, Drickamer, and dePasquali[56] have suggested a similar volume dependence for $\rho_{\text{Fe}}(0)$ for metallic iron with $\gamma_{\text{Fe}} = 1.25$.

Combining Eqs. (1), (16a), and (17), the isomer shift ΔE for a binary gold alloy may be written as

$$\Delta E = Kn\rho_{\text{Au}}(0)\{(v_{\text{Au}}/v)^{\gamma}[1 + \textstyle\sum_i m_X c_i(1-\alpha_i)\,\bar{\rho}_{x,s}(r_i)] - 1\}\,. \tag{18}$$

This expression gives an explicit dependence of ΔE on volume, composition, and order parameters. The value which we will determine for $\bar{\rho}_{x,s}(r_i)$ in Sec. V will be a mean value for the entire alloy composition range. The physical interpretation of the quantity $\bar{\rho}_{x,s}(r_i)$ is as follows: If in an alloy sample of pure gold, one gold atom is replaced by an x atom, $\bar{\rho}_x(r_i)/\rho_{\text{Au}}(0) = (V_{\text{Au}}/V)^{\gamma}\,\bar{\rho}_{x,s}(r_i)$ gives the fractional change of charge density at the gold nuclei in the ith shell of gold neighbors at distance r_i surrounding the x site. $\bar{\rho}_x(r_i)/\rho_{\text{Au}}(0)$ is the quantity which through our approximate W-S model [Eq. (18)] specifically describes the order dependence of the isomer shift of gold in the alloy. As we have indicated in Sec. I our measurements are interpreted to give information about this fractional charge density $\bar{\rho}_x(r_i)/\rho_{\text{Au}}(0)$ and also about the volume-dependent contribution $\bar{\rho}_a(0)$ [Eq. (14)]. In this model [Eq. (18)], the volume dependence of $\rho_{\text{alloy}}(0)$ will thus be entirely due to the factor $(V_{\text{Au}}/V)^{\gamma}$ and the composition and order dependence will be described by the term in $\langle n_x\rangle_i$.

V. COMPARISON OF ISOMER-SHIFT MODEL WITH EXPERIMENT

A. Alloys of Gold with Silver

The atomic volumes of gold and silver metals are nearly the same and the average atomic volume of the alloys is close to v_{Au}. Thus we shall take $v_{\text{Au}}/v = 1$. In so far as the Au-Ag alloys are completely disordered, the α_i will be equal to zero.

Then for gold in silver, Eq. (18) gives

$$\Delta E = 8 m_{\mathrm{Ag}} \sum_i c_i \bar{\rho}_{\mathrm{Ag},s}(r_i) \text{ mm/sec} , \quad (19)$$

where the value $Kn\rho_{\mathrm{Au}}(0) = 8$ mm/sec has been used and m_{Ag} is the atomic fraction of silver atoms. This equation then describes the observed linear dependence of ΔE on m_{Ag} in Fig. 6 and gives the result that

$$\sum_i c_i \bar{\rho}_{\mathrm{Ag},s}(r_i) \cong 0.27 . \quad (20)$$

The composition dependence of the isomer shift in the silver alloys is due predominantly to scattering at the silver-ion sites. There is no appreciable dependence of ΔE on alloy volume in this case.

B. Alloys of Gold with Copper

For the Au-Cu alloy system, v_{Au}/v ranges from 1 to ~ 1.3 with composition, and the order parameters are not negligible when compared with unity [Table I]. A knowledge of the dependence of ΔE, v_{Au}/v, and of α_i on composition and heat treatment then enables one to obtain information for the Cu-Au system about $\bar{\rho}_{\mathrm{Cu},s}(r_i)$.

We have given measured values for ΔE in Sec. III. Values for v_{Au}/v have been given by Dienes [4] [Table I]. One approximate value for α_i has been obtained[7] by x-ray methods for the composition Cu_3Au for the disordered system $T_Q = 800\,^{\circ}\mathrm{C}$ [Table I]. Also given in this table are approximate values of α_1 and α_2 for various compositions of ordered Cu-Au alloys calculated as described above from a theoretical model given by Cowley.[5]

For the purpose of comparing Eq. (18) to our isomer-shift measurements for the 23 ordered Au-Cu alloys we have assumed that the mean value $\bar{\rho}_{\mathrm{Cu},s}(r_i)$ could be described in terms of a Taylor expansion for each shell of neighbors i, as follows:

Nearest-neighbor shell:

$$\bar{\rho}_{\mathrm{Cu},s}(r_i) = \bar{\rho}_{\mathrm{Cu},s}\left(\frac{a}{\sqrt{2}}\right) + \left(r_1 - \frac{a}{\sqrt{2}}\right)\frac{d}{dr_1}\bar{\rho}_{\mathrm{Cu},s}(r_1)\Big|_{a/\sqrt{2}} + \cdots ;$$

next-nearest-neighbor shell:

$$\bar{\rho}_{\mathrm{Cu},s}(r_2) = \bar{\rho}_{\mathrm{Cu},s}(a) + \cdots ; \quad (21)$$

all other shells:

$$\bar{\rho}_{\mathrm{Cu},s}(r_i) = 0, \quad \text{for } i \geq 3 .$$

In these Taylor[57] expansions we have kept only the first two terms for the nearest-neighbor shell, and we have retained only the first term for the second-nearest-neighbor shell. It has been assumed as indicated in Eqs. (21) that the contributions from all of the more remote shells of neighbors are relatively small and these terms have been omitted.[58] In Eqs. (21), the Taylor expansion for each shell has been made around the corresponding shell radius for pure gold, $a/\sqrt{2}$ for nearest neighbors, and a for the next-nearest neighbors. Here a is the lattice parameter for pure gold, $a = 4.064$ Å. In this approximation we have retained three adjustable constants. Values for these constants in Eqs. (22) have been obtained by fitting Eqs. (18) and (21) to the isomer-shift values determined experimentally for the cases of ordered CuAu ($c_1 = 12$, $\alpha_i = -\frac{1}{3}$, $c_2 = 6$, $\alpha_2 = 1$), ordered Cu_3Au ($c_1 = 12$, $\alpha_1 = \frac{4}{3}$, $c_2 = 6$, $\alpha_2 = 1$), and for a vanishing concentration of Au in Cu ($c_1 = 12$, $\alpha_1 = 0$, $c_2 = 6$, $\alpha_2 = 0$). Again the value for $Kn\rho_{\mathrm{Au}}(0) = 8.0$ mm/sec has been used:

$$\bar{\rho}_{\mathrm{Cu},s}(a/\sqrt{2}) = 0.0184 , \quad (22a)$$

$$\frac{d}{dr_1}\bar{\rho}_{\mathrm{Cu},s}(r_1)\Big|_{r_1 = a/\sqrt{2}} = 0.0212 \text{ Å}^{-1} , \quad (22b)$$

$$\bar{\rho}_{\mathrm{Cu},s}(a) = -0.0059 . \quad (22c)$$

The solid curve of Fig. 4 shows the fit of Eq. (18) to the experimental data for the ordered alloys where the values of the three constants in Eqs. (22) have been used in the Taylor expansion for $\rho_{\mathrm{Cu},s}(r_i)$ in Eqs. (21). In this fit the values of α_i and (v_{Au}/v) used are those given in Table I. The model is seen to fit the data quite well except perhaps in the vicinity of 40% Au, where the departure is ~ 0.05 mm/sec. As was noted in Sec. IIC, however, the calculation of the order parameters through our use of the Cowley model is least certain near this composition.

The interpretation of the constants in Eqs. (22) is as follows: If an atom of gold in the pure metal is replaced by an atom of copper, the charge density at the nearest-neighbor gold nucleus [Eq. (22a)] is increased by 1.8% and the charge density at the second-nearest-neighbor gold site is decreased by 0.6%.

Friedel,[59] Daniel,[60] Blandin and Daniel,[61] Harrison,[52] and others have previously suggested that oscillations of this nature will occur due to the screening electron charge density about a point charge in a nearly-free-electron gas. Clapp and Moss[6] have indirectly observed effects of these oscillations for the cases of Cu_3Au, CuAu, and $CuAu_3$ by studying the interaction energies between pairs of neighboring atoms in the CuAu alloys.

Referring back to Eqs. (4)–(6), one may see that the small quantities $\bar{\rho}_{\mathrm{Cu},s}(r_i)$ come predominantly from the cross term between the incident and scattered waves [Eq. (6c)]. Since the amplitude of the incident wave is of order 1, the neglected terms will be of the order $[\bar{\rho}_{\mathrm{Cu},s}(r_i)]^2 \sim 10^{-4}$. Thus the interference terms neglected are in fact small in comparison to the terms retained, and also compared to our experimental error.

Using the values of $\bar{\rho}_{\mathrm{Cu},s}(r_i)$ as determined by

Eqs. (21) and (22), we may compute a sum for the Cu-Au alloys similar to the expression in Eq. (20) for Ag-Au. For r_i near the pure gold values

$$\sum_i c_i \bar{\rho}_{\mathrm{Cu},s}(r_i) = 0.186, \tag{23a}$$

and for r_i near the pure copper values

$$\sum_i c_i \bar{\rho}_{\mathrm{Cu},s}(r_i) = 0.103\ . \tag{23b}$$

Thus for the Cu-Au alloys the contribution to the isomer shift due to scattering at the copper sites is interpreted to be somewhat less than the similar term for Ag-Au alloys. On the other hand, volume effects are stronger in the Cu-Au alloys.

For an infinitely dilute solution of gold in copper, ΔE relative to pure gold is (4.049 ± 0.005) mm/sec. Of this, the contribution due to scattering effects, Eq. (18),

$$\Delta E_{\mathrm{scattering}} = Kn\rho_{\mathrm{Au}}(0)\,(v_{\mathrm{Au}}/v)^{\gamma} \times \sum_i m_{\mathrm{Cu}} c_i (1-\alpha_i)\bar{\rho}_{\mathrm{Cu},s}(r_i) \tag{24}$$

can be evaluated through the constants given in Eqs. (21) and (22). For this infinitely dilute case, then [Table I] Eq. (24) gives $\Delta E_{\mathrm{scattering}}$ = 1.113 mm/sec, which accounts for about one-fourth of the total isomer shift. Similarly, the contribution to the isomer shift ΔE due to volume effects,

$$\Delta E_{\mathrm{volume}} = Kn\rho_{\mathrm{Au}}(0)\,[(v_{\mathrm{Au}}/v)^{\gamma} - 1]\ , \tag{25}$$

can be evaluated for the infinitely dilute case as $\Delta E_{\mathrm{volume}}$ = 2.931 mm/sec. Here, the effect of compression accounts for about three-fourths of the total isomer shift.

Referring to Fig. 3, the contribution to the isomer shift due to compression [Eq. (25)] has been computed for each composition and is shown as the curve marked $\Delta E_{\mathrm{volume}}$. Similarly, the contribution to the isomer shift due to scattering from copper lattice sites $\Delta E_{\mathrm{scattering}}$ is computed from Eq. (24). Finally, in Fig. 3, we have indicated by curve $\Delta E_{\mathrm{random}}$ the isomer shift which would be expected for a totally disordered alloy ($\alpha_i = 0$ for all i). This function is given by Eq. (18) with $\alpha = 0$.

The agreement shown in Fig. 4 between Eqs. (18) and (22) and the experimental data is close. Qualitatively the double-peak structure of the theoretical curve is due to the character of the Cowley model,[5] Eqs. (3e), for the order parameters α_i.

C. Quench Temperature Dependence of Isomer Shift for Cu_3Au

Since the dominant contribution to the isomer shift observed for Cu-Au alloys is the volume term in Eq. (25), it is important to note that the dependence of lattice volume on short-range order is quite small in the case of Cu_3Au. For example, the change of volume[4] between the ordered state and the disordered state is $(\Delta v/v) \approx 0.001$ [Table I]. Using this number in Eq. (25) we find an isomer-shift change of 0.01 mm/sec, which is approximately our experimental error. Thus, the change of ΔE with T_Q for Cu_3Au given in Fig. 5 is due predominantly to changes in $\Delta E_{\mathrm{scattering}}$ with short-range order.

As stated previously, only one measurement of α_i has been made for Cu-Au alloys quenched from high temperature. The measurement was made for Cu_3Au by Moss[7] [Table I] for a sample quenched from 800 °C. His values of α_i have been used in Eq. (18) to obtain a value of ΔE which is plotted as an x in Fig. 5. The agreement with our isomer-shift measurements is within ~ 3.5%.

D. Pressure Dependence of Isomer Shift for an Alloy

A further check on Eq. (18) may be obtained by a study of the pressure dependence of the isomer shift for alloys. From Eq. (18), the change of the isomer shift with pressure $\delta\Delta E_p$ is given by

$$\delta\Delta E_p = Kn\rho_{\mathrm{Au}}(0)\gamma\,[1 + \sum_i m_x c_i (1-\alpha_i)\bar{\rho}_{\mathrm{Cu},s}(r_i)](\Delta v/v_0)\ , \tag{26}$$

where v_0 is the average atomic volume of the alloy. We have measured $\delta\Delta E_p$ for[12] Au and for ordered Cu_3Au.

With the results of Tables I and II, Eqs. (22) and (26), and Sec. III D, we may calculate $\delta\Delta E_p$ for ordered Cu_3Au at 65 kbars. We thus obtain a calculated value of $\delta\Delta E_p$ = 0.33 mm/sec. This may be compared with the measured value in Table II of $\delta\Delta E_p$ = (0.32 ± 0.03) mm/sec. Thus, within the experimental error of ~ 10%, Eqs. (18) and (26) describe this high-pressure result. Since $Kn\rho_{\mathrm{Au}}(0)$ is a constant, γ is, within experimental error, the same for Cu_3Au and for pure gold.[12]

ACKNOWLEDGMENTS

We are grateful to K. Dy, G. Czjzek, F. E. Obenshain, and John Burton for helpful discussions of this work.

†Research jointly sponsored by the U. S. Atomic Energy Commission under contract with the Union Carbide Corporation and under contract AT-(40-1)-3897 with the University of North Carolina, by the University of Tennessee, and by the Advanced Research Projects Agency, contract SD100 at the University of North Carolina. This paper is based in part on a dissertation submitted by Paul G. Huray to the faculty of the University of Tennessee, Knoxville, Tenn., in partial fulfillment of the requirement for the Ph. D. degree in physics.

*Dissertation work performed as an Oak Ridge Graduate Fellow from the University of Tennessee under appoint-

ment with Oak Ridge Associated Universities from 1966 to 1968. Present address: Physics Department, University of Tennessee, Knoxville, Tenn. 37916.

‡Present address: Physics Department, University of North Carolina, Chapel Hill, N. C. 27514.

[1]R. L. Mössbauer, Z. Physik 151, 125 (1958); Naturwiss. 45, 538 (1958).

[2]C. H. Johansson and J. O. Linde, Ann. Physik 25, 17 (1936).

[3]M. Hansen and K. Anderko, *Constitution of Binary Alloys* (McGraw-Hill, New York, 1958); R. P. Elliott, *Constitution of Binary Alloys, First Supplement* (McGraw-Hill, New York, 1965).

[4]G. A. Dienes, Acta Met. 6, 278 (1958).

[5]J. M. Cowley, Phys. Rev. 77, 669 (1950); 120, 1648 (1960).

[6]P. C. Clapp and S. C. Moss, Phys. Rev. 142, 418 (1966); 171, 754 (1968); 171, 674 (1968).

[7]S. C. Moss, J. Appl. Phys. 35, 3547 (1964).

[8]S. Siegel, *Phase Transformations in Solids* (Wiley, New York, 1951), p. 366; A. Guinier and R. Griffoul, Compt. Rend. 221, 555 (1945); A. Guinier, Proc. Phys. Soc. (London) 57, 310 (1945).

[9]O. Nygaard and L. Vegard, Skrifter Norske Videnskaps-Akad. Oslo, I. Mat. Naturv. Kl. 2, 37 (1947); Structure Repts. 11, 126 (1947).

[10]C. S. Smith, Mining and Metallurgy 9, 458 (1928).

[11]Louis D. Roberts, Richard L. Becker, F. E. Obenshain, and J. O. Thomson, Phys. Rev. 137, A895 (1965).

[12]Louis D. Roberts, D. O. Patterson, J. O. Thomson, and R. P. Levey, Phys. Rev. 179, 656 (1969); D. O. Patterson, thesis (University of Tennessee, 1968) (unpublished).

[13]D. O. Patterson, J. O. Thomson, P. G. Huray, and Louis D. Roberts, Phys. Rev. B 2, 2440 (1970); D. O. Patterson, thesis (University of Tennessee, 1968) (unpublished).

[14]R. Feder, M. Mooney, and A. S. Nowick, Acta Met. 6, 226 (1958).

[15]F. E. Jaumot and C. H. Sutcliffe, Acta Met. 2, 63 (1954).

[16]B. E. Warren and D. T. Keating, J. Appl. Phys. 22, 286 (1951).

[17]T. J. Rowland, Phys. Rev. 119, 900 (1960); 125, 459 (1962); 134, A743 (1964).

[18]W. T. Anderson, F. C. Thatcher, and R. R. Hewit, Phys. Rev. 171, 541 (1968).

[19]L. C. Alfred and D. O. Van Ostenberg, Phys. Rev. 161, 569 (1967).

[20]W. Kohn and S. H. Vosko, Phys. Rev. 119, 912 (1960).

[21]R. L. Odle and C. P. Flynn, Phil. Mag. 13, 699 (1966); J. Phys. Chem. Solids 26, 1685 (1965); D. A. Rigney and C. P. Flynn, Phil. Mag. 15, 1213 (1967); C. P. Flynn and E. F. W. Seymour, Proc. Phys. Soc. (London) 76, 526 (1960).

[22]Albert Narath and H. T. Weaver, Phys. Rev. 175, 373 (1968); Albert Narath, *ibid.* 163, 232 (1967).

[23]L. H. Bennett, R. W. Mebs, and R. E. Watson, Phys. Rev. 171, 611 (1968).

[24]Wen Lin, R. O. Williams, and J. E. Spruiell, J. Appl. Cryst. 3, 297 (1970).

[25]R. Brill, in *Solid State Physics*, edited by F. Seitz, D. Turnbull, and H. Ehrenreich (Academic, New York, 1967), Vol. 20.

[26]B. Borie and B. E. Warren, J. Appl. Phys. 27, 1562 (1956).

[27]H. Frauenfelder, *The Mössbauer Effect* (Benjamin, New York, 1963).

[28]O. C. Kistner and A. W. Sunyar, Phys. Rev. Letters 4, 412 (1960).

[29]L. R. Walker, G. K. Wertheim, and V. Jaccarino, Phys. Rev. Letters 6, 98 (1961).

[30]D. Nagle, P. P. Craig, J. G. Dash, and R. R. Reiswig, Phys. Rev. Letters 4, 237 (1960).

[31]D. A. Shirley, Phys. Rev. 124, 354 (1961); D. A. Shirley, M. Kaplan, and P. Axel, *ibid.* 123, 816 (1961).

[32]D. A. Shirley, Science 161, 745 (1968); D. A. Shirley, R. W. Grant, and D. A. Keller, Rev. Mod. Phys. 36, 352 (1964).

[33]P. Steiner, E. Gerdau, W. Hautsch, and D. Steenken, in *Hyperfine Structure and Nuclear Radiations*, edited by E. Matthias and D. A. Shirley (North-Holland, Amsterdam, 1968).

[34]Louis D. Roberts and J. O. Thomson, Phys. Rev. 129, 664 (1963).

[35]G. Longworth, J. Phys. C: Metal Phys. Suppl. No. 1, S81 (1970).

[36]R. L. Cohen, Phys. Rev. 171, 343 (1968); Phys. Rev. B 3, 2872 (1971).

[37]B. D. Dunlap, J. B. Darby, and C. W. Kimball, Phys. Letters 25A, 431 (1967).

[38]M. O. Faltens, thesis (University of California, Berkeley, 1969) (unpublished).

[39]Paul G. Huray, Louis D. Roberts, and J. O. Thomson, in *Hyperfine Structure and Nuclear Radiations*, edited by E. Matthias and D. A. Shirley (North-Holland, Amsterdam, 1968).

[40]Paul G. Huray, thesis (University of Tennessee, 1968) (unpublished).

[41]R. S. Preston, S. S. Hanna, and J. Heberle, Phys. Rev. 128, 2207 (1962).

[42]P. Cziffra and M. J. Moravcsik, Lawrence Radiation Laboratory Report UCRL-8523 (unpublished).

[43]D. J. Erickson, Louis D. Roberts, J. W. Burton, and J. O. Thomson, Phys. Rev. B 3, 2180 (1971).

[44]W. L. Bragg and E. J. Williams, Proc. Roy. Soc. (London) A145, 699 (1934).

[45]B. W. Roberts, Acta Met. 2, 597 (1954); B. W. Batterman, J. Appl. Phys. 28, 556 (1957).

[46]M. A. Krivoglaz and A. A. Smirnov, *The Theory of Order-Disorder in Alloys* (American Elsevier, New York, 1965).

[47]F. N. Rhines, W. E. Bond, and R. A. Rujmel, Trans. ASM 47, 578 (1955).

[48]W. Schule, thesis (Max Planck Institut für Metallforschung, Stuttgart, 1957) (unpublished).

[49]H. Hirabayaski, S. Nagaskai, and H. Kono, J. Appl. Phys. 28, 1070 (1957).

[50]K. A. Gschneider, Jr., in *Solid State Physics*, edited by F. Seitz and D. Turnbull (Academic, New York, 1964), Vol. 16, p. 275.

[51]P. A. Flinn, G. M. McManus, and J. A. Rayne, J. Phys. Chem. Solids 15, 189 (1960).

[52]W. A. Harrison, *Pseudopotentials in Theory of Metals* (Benjamin, New York, 1966).

[53]W. H. Young, A. Meyer, and G. E. Kilby, Phys. Rev. 160, 482 (1967).

[54]Thomas C. Tucker, Louis D. Roberts, C. W. Nestor, Jr., and Thomas A. Carlson, Phys. Rev. 178, 998 (1969).

[55]R. Ingalls, Phys. Rev. 155, 157 (1967).

[56]R. Ingalls, H. G. Drickamer, and G. DePasquali, Phys. Rev. 155, 165 (1967).

[57]B. Taylor, *Methodus Incrementorum Directa et Inversa* (London, 1715).

[58]The model which we have used for the order parameters should be a quite good approximation for the α_i near the compositions Au, CuAu, Cu_3Au, and for dilute solutions of Au in Cu. At other compositions the estimates for the α_i will be more approximate. The use of the α_i at the above four compositions permits us to estimate $\bar{\rho}_{Cu,s}(r_i)$ for $i=1,2$. $\bar{\rho}_{Cu,s}(r_i)$ could be obtained for $i \geq 3$ from our data if reliable α_i were available for other concentrations. Until a more complete treatment of the α_i as a function of composition is obtained, we will interpret our measurements in terms of nearest- and next-nearest-neighbor shells only. As will be seen in Fig. 4, the fit of our model to the isomer-shift measurements is close. The results of Clapp and Moss[6] for the interatomic potential $V_{AB}(r_i)$ indicate that $V_{AB}(r_3)=0$ for the Cu-Au alloys. Correspondingly, the contribution of third neighbors to the order dependence of the isomer shift may also be small, as we assume here.

[59]J. Friedel, J. Phys. Radium 23, 392 (1962); Phil. Mag. 43, 153 (1952).

[60]E. Daniel, J. Phys. Chem. Solids 10, 174 (1959).

[61]A. Blandin and E. Daniel, J. Phys. Chem. Solids 10, 126 (1959).